International Research Journal of Engineering and Technology (IRJET) e-ISSN: 2395-0056
Volume: 08 Issue: 10 | Oct 2021 www.irjet.net p-ISSN: 2395-0072

Energy Differential and Double Differential Cross-Section Calculation of Charged Particle Emission for Natural Molybdenum

Navita[1], G.C. Joshi[2], Bhawna Pandey[1]

[1]*Department of Physics, G. B. Pant University of Agriculture & Technology, Pantnagar, Uttarakhand, India*
[2]*Department of Physics,* Radiations and Tracers Laboratory, *G. B. Pant University of Agriculture & Technology, Pantnagar, Uttarakhand, India*

Abstract - *Molybdenum is considered as one of the important plasma facing materials (PFM) for the development of fusion reactor. Energy differential and double differential cross-section data is crucial to estimate material damage. In the present study, energy differential and double differential cross-section data of emitted proton and alpha particles induced by (n,xp) and (n,xα) nuclear reactions for the natural molybdenum at 14.1 MeV neutron energy have been calculated at 10º, 30º, 60º, 90º and 120º angles using suitable nuclear models in TALYS-1.9. The computation of energy differential cross-section indicates that most of proton and alpha particles emitted by (n,xp) and (n,xα) nuclear reactions for the natural molybdenum are of 5 MeV and 13MeV, respectively.*

Key Words: **Plasma facing materials, Energy differential cross-section, double differential cross-section, TALYS-1.9, molybdenum**

1.Introduction

The construction of fusion power reactors would place very demanding operating conditions on plasma facing materials (PFMs). The PFMs are worked in an environment which incorporates high energy incident particles and heat flux from the plasma. The PFMs' surface is exposed to degradation because of energetic neutrons and ions fleeing from plasma **(1,2)**. PFMs with high performance under harsh environmental conditions should be designed in order to construct next-generation fusion reactors **(3).** The evaluation of nuclear heating and material damage of the structural materials of the candidate reactors is very important in the development of fusion reactors. One of the key data for these estimates is the energy distribution and angular distribution of charged particles (proton, deuteron, alpha particle etc.) emitted as a result of neutron impact on the reactor equipments, particularly the blanket and first wall. Therefore, accurate differential double differential cross-section data plays crucial role in the design of the reactor structural materials. **(4)**

High melting point (2623ºC), low erosion rate and good thermal properties and some of the prominent properties of Molybdenum which make it promising candidate for PFM in the fusion reactor **(3).** Molybdenum is considered as first wall material in fusion reactor (**5).** Even at high temperature, molybdenum is one of the excellent structural materials. As a result, it has a great potential for use in neutronic applications such as controlled nuclear fusion reactor **(6).**

In the present study, energy differential and double differential cross-section data of emitted proton and alpha particles for the natural molybdenum plasma facing material have been calculated.

Molybdenum has seven stable isotopes i.e. ^{92}Mo, ^{94}Mo, ^{95}Mo, ^{96}Mo, ^{97}Mo, ^{98}Mo and ^{100}Mo and their respective abundance is 14.65%, 9.19%, 15.87%, 16.67%, 9.58%, 24.29% and 9.74%. As the importance of Molybdenum is already discussed, molybdenum may be utilized in its natural state in the upcoming fusion reactor ITER.

2. Materials and methods

The estimation of nuclear reactions plays a significant role in the cross-section assessment due to insufficient experimental evidence in the literature **(7).** Energy differential and double differential cross-section for the stable isotopes of molybdenum have been calculated using computer based nuclear reaction modular code TALYS-1.9 **(8).**

Basically TALYS-1.9. is one of the powerful nuclear modular codes to predict reaction cross-section mechanism by using different models such as pre-equilibrium, compound, direct, optical model, fission, statistical nuclear reaction model and provides a forecast for all open reaction channels. For TALYS-1.9 involves photons, protons, neutron, deuterons, tritons, alpha and ^{3}He as incident particles in the energy range from 0.001 MeV to 200 MeV and the mass number (A) of the target nuclei can be vary from 12 to 399.

The magnitude and the shapes of the excitation functions from 0 MeV to 20 MeV are described by level density model calculations using a set of default parameters in TALYS 1.9. On the basis of different reaction mechanisms, such as preequilibrium emission, direct reactions and compound nucleus reaction, the code provides precise and complete information of reaction cross-sections. The default parameters for direct, pre-equilibrium and compound nucleus reaction calculation are optical model, Exciton model and Hauser-Feshbach model with Moldauer width fluctuation correction respectively. Nuclear level densities play crucial role during nuclear reaction calculation.

Various level density models have been used to optimize input parameters. The models for level density used in TALYS-1.9 are given below:

i. Ldmodel1: Constant temperature and Fermi-gas model (CTFM), in which the constant temperature model is implemented for the low excitation energy range and the Fermi-gas model is implemented for the high excitation energy range.
ii. Ldmodel2: Back-shifted Fermi-gas model (BSFM).
iii. Ldmodel3: Generalized superfluid model (GSM).
iv. Ldmodel4: Microscopic level densities (skyrme force) from Goriely's table.
v. ldmodel5: Microscopic level densities (skyrme force) from Hilaire's combinatorial tables.
vi. Ldmodel6: Microscopic level densities (temperature dependent HFB, Gogny force) from Hilaire's combinatorial table.

Koning and Delaroche proposed local optical model. This model is implemented in TALYS-1.9 for the calculation of direct reaction. Contribution of Compound nuclear reaction to EDX data has been calculated using the Hauser-Feshbach model and is given by the following formula **(9)**

$$\frac{d\sigma}{dE} = \sum_{j\pi} \sigma CN\,(E_a)\,\frac{\sum_{l\pi}\Gamma\, b(U,J,\pi,E,I,\pi)\rho b(E,I,\pi)}{\Gamma(U,J,\pi)}$$

Where 'a' represents projectile particle while 'b' represents ejectile particle. σCN represents the production cross-section of compound nucleus for projectile having energy Ea, Γ_b is the transmission coefficient for ejectile 'b', ρb(E,I,Π) is the nuclear level density of the residual nuclei, (E,I,Π) and (U,J,Π) represents energy, angular momentum and parity of residual and compound nucleus, respectively.

On the other hand, Pre-equilibrium reaction has been evaluated using the two-component exciton method of Kalbach **(10)**. and given by the formula,

$$\frac{d\sigma}{dE} = \sigma^{CF} \sum_{p_\pi=p_\pi^0}^{p_\pi^{eq}} \sum_{p_n=p_n^0}^{p_n^{eq}} \omega_k(p_\pi,h_\pi,p_n,h_n,E_k) S_{pre}(p_\pi,h_\pi,p_n,h_n,E_k)$$

Kalbach method **(10)** has been used to calculate DDX and given by following formula –

$$\frac{d^2\sigma_{i,k}}{dE_k d\Omega} = \frac{1}{4\Pi}\left[\frac{d\sigma^{PE}}{dE_k} + \frac{d\sigma^{comp}}{dE_k}\right]\frac{b}{sinhb} \times \left(cosh(bcos\theta) + f_{MSD}(E_k)sinh(bcos\theta)\right)$$

Where f_{MSD} is called multi-step ratio and given by

$$f_{MSD} = \frac{d\sigma^{PE}}{dE_k} \Big/ \left[\frac{d\sigma^{PE}}{dE_k} + \frac{d\sigma^{copm}}{dE_k}\right]$$

The nuclear model variables were optimized by comparing the computed (n, p) and (n, α) reaction cross-sections from TALYS-1.9 with experimental data from the EXFOR data set for all stable Molybdenum isotopes and then the same nuclear parameters have been used for calculating energy differential and double differential cross-section for the stable isotopes of Molybdenum.

3. Result and discussion

For (n,xp) and (n,xα) reaction pathwayss, EDXs and DDXs are calculated for the seven stable isotopes of Molybdenum. To calculate EDX and DDX for natural molybdenum, input data are optimized by comparing experimental cross-sectional data of all the stable isotopes of molybdenum with calculated cross-sections.

3.1 (n,p) and (n, α) reaction cross-section of ^{92,98}Mo

To optimize input parameters, (n, p) and (n, α) reaction cross-section of all the stable isotopes of molybdenum has been compared with the experimental data present in EXFOR data library. In figure 1, 2,3 and 4, we have shown the computed excitation function of ^{92,98}Mo(n,p) and ^{92,98}Mo(n, α) with experimental data. Similarly, (n,p) and (n,α) reaction

cross-section for all other stable isotopes of molybdenum has been calculated.

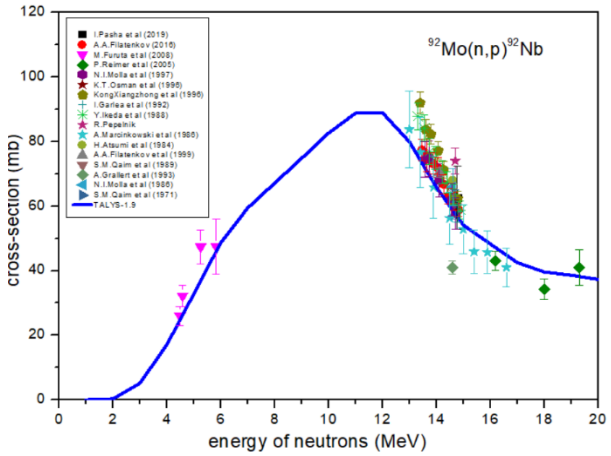

Fig-1: Cross section of ^{92}Mo(n, p) ^{92}Nb reaction.

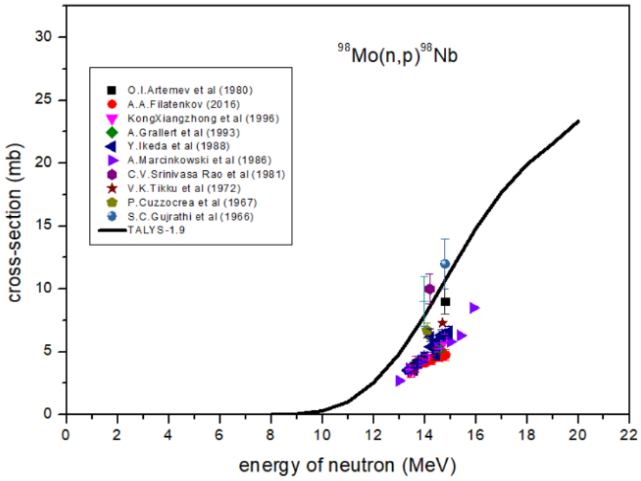

Fig-2: Cross section of ^{98}Mo(n, p) ^{98}Nb reaction.

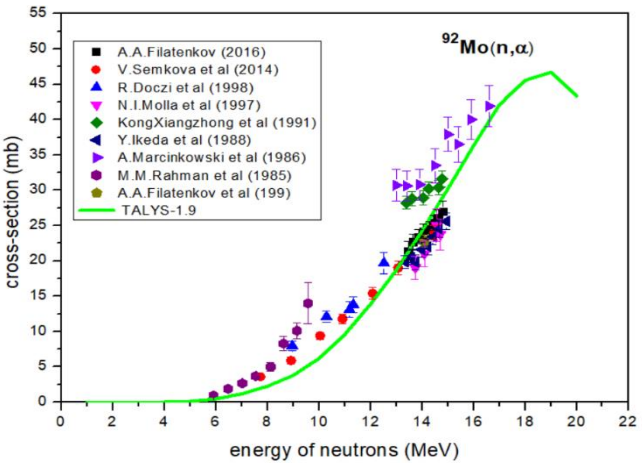

Fig-3: Cross section of ^{92}Mo(n, α) ^{89}Zr reaction.

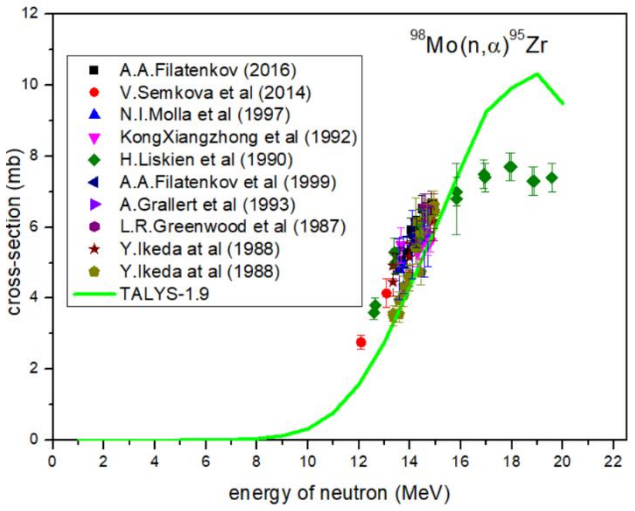

Fig 4: Cross section of ^{98}Mo(n, α) ^{95}Zr reaction.

3.2 EDX for (n,xp) and (n,xα) reaction on ^{92,94,95,96,97,98,100}Mo

The calculated EDX for (n,xp) reactions on all the stable isotope of molybdenum are shown in figure 5, 6, 7, 8, 9, 10 and 11. The contribution of different reaction mechanism i.e. direct, compound and pre-equilibrium reaction is also shown in respective figures. There is no experimental data available in EXFOR for molybdenum regarding EDX at 14.1MeV energy of neutrons.

From the calculation of EDX for ^{92}Mo(n,xp) reaction which is shown in fig. 5, it is observed that compound reaction majorly contributes to the energy spectrum of outgoing protons while contribution of pre-equilibrium and direct reaction is negligible to total EDX. The contribution of direct reaction is least significant. ^{94}Mo(n,xp) reaction, as shown in fig. 6, is also proceed through compound reaction mechanism. The contribution of pre-equilibrium reaction is also appreciable while the emission of proton via direct reaction mechanism is negligibly low.

EDX for ^{95,96,97,98,100}Mo(n,xp) is shown in fig. 7, 8, 9, 10 and 11, respectively. From the figures, it is obvious that the energy spectra of proton emission from ^{95,96,97,98,100}Mo(n,xp) reactions are proceeds mainly via pre-equilibrium reaction mechanism. The contribution of direct reaction mechanism is also started to come into the pictures at higher energy of proton emission and the contribution of compound reaction mechanism to the total EDX is appreciable only at the low emission energy of protons.

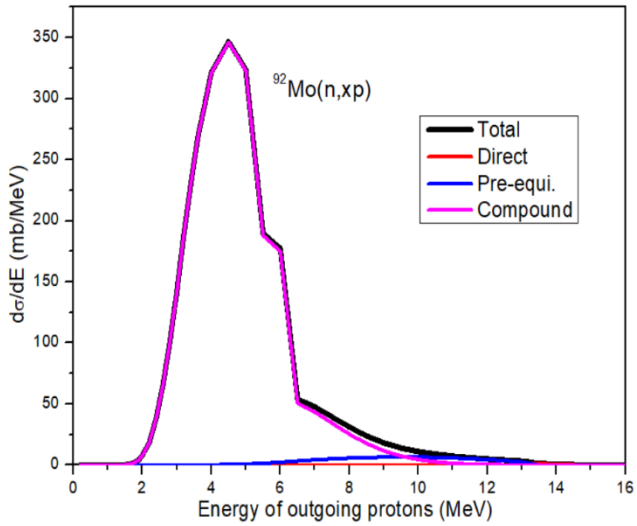

Fig-5: EDX of (n, xp) reaction on ^{92}Mo at 14.1 MeV neutron energy.

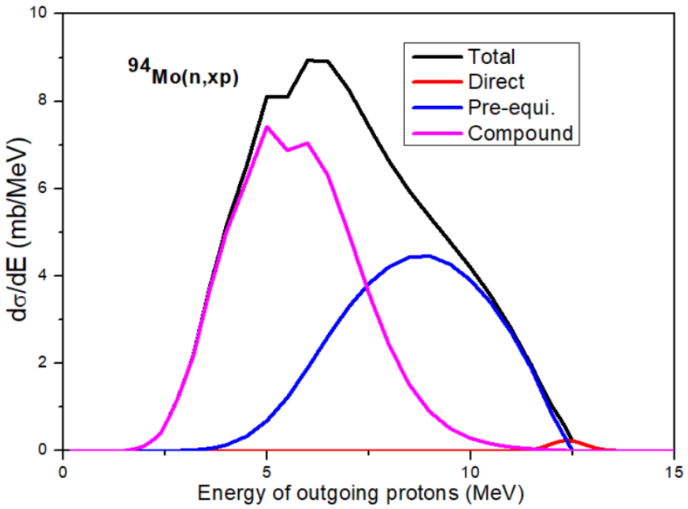

Fig-6: EDX of (n, xp) reaction on ^{94}Mo at 14.1 MeV neutron energy.

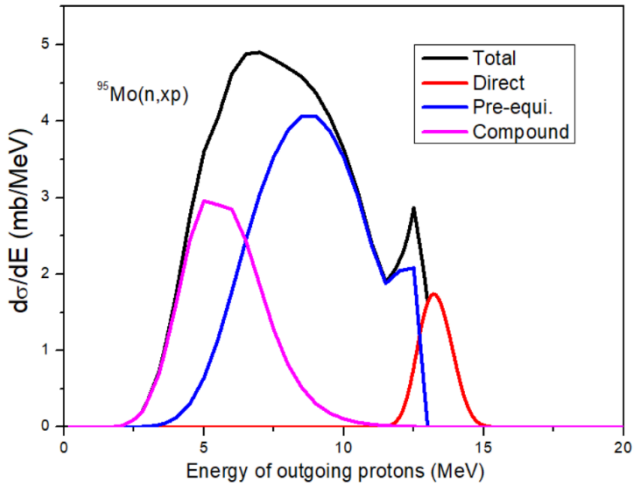

Fig-7: EDX of (n, xp) reaction on ^{95}Mo at 14.1 MeV neutron energy.

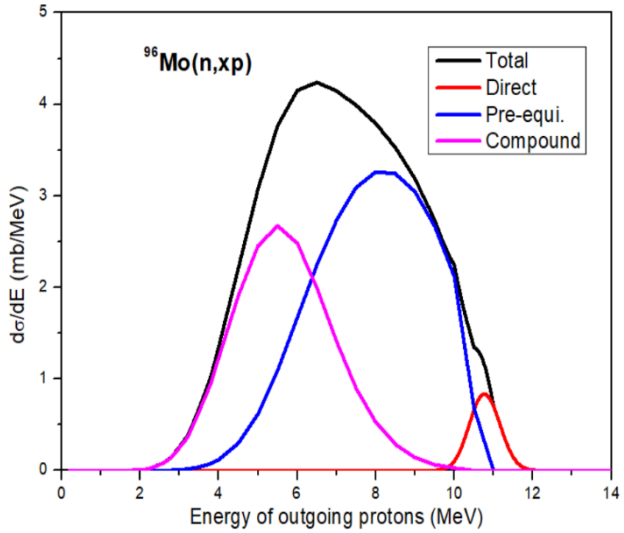

Fig-8: EDX of (n, xp) reaction on ^{96}Mo at 14.1 MeV neutron energy.

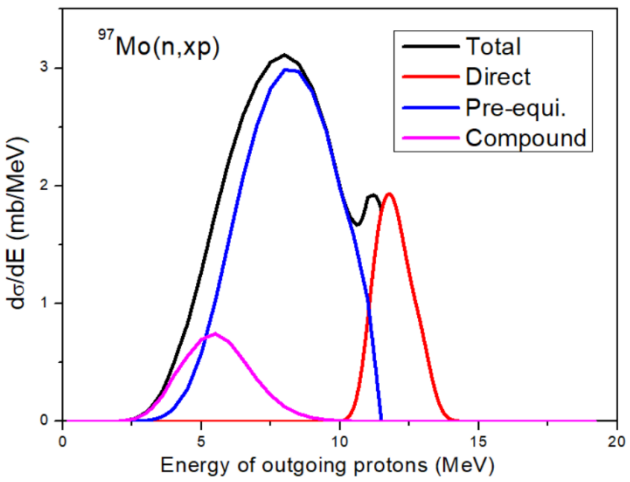

Fig-9: EDX of (n, xp) reaction on ^{97}Mo at 14.1 MeV neutron energy.

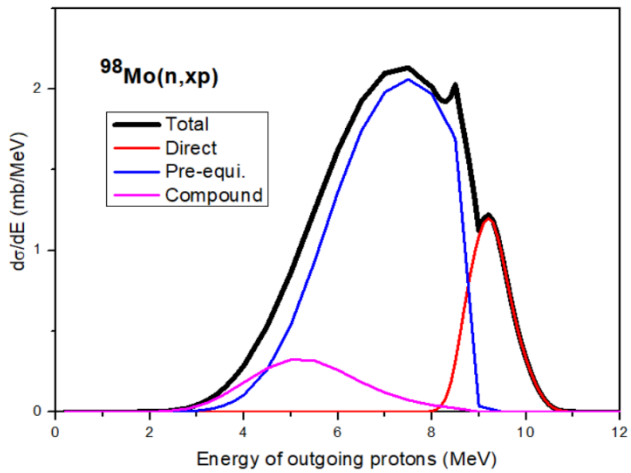

Fig-10: EDX of (n, xp) reaction on ^{98}Mo at 14.1 MeV neutron energy.

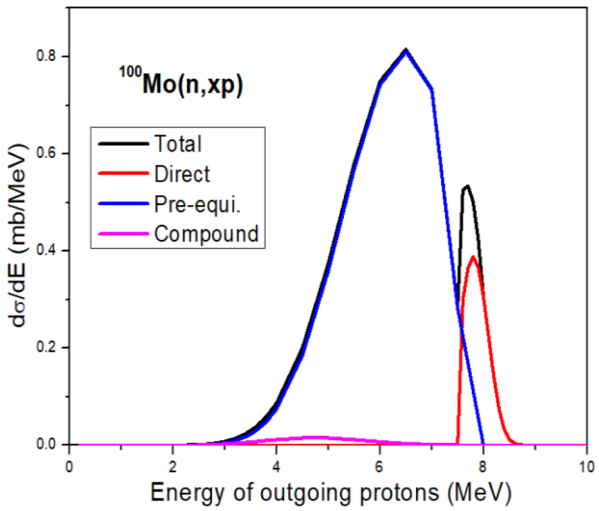

Fig-11: EDX of (n, xp) reaction on ^{100}Mo at 14.1 MeV neutron energy.

EDX calculation for ^{92,94,95,96,97,98,100}Mo(n,xα) reactions are shown in figure 12, 13, 14, 15, 16, 17 and 18 respectively. Energy spectra of ^{92}Mo(n,xα) in fig.12 shows that the reaction mainly proceeds through compound reaction while pre-equilibrium reaction dominates for ^{94,95,96,97,98,100}Mo(n,xα) reactions and contribution of direct reactions is either low or negligibly small.

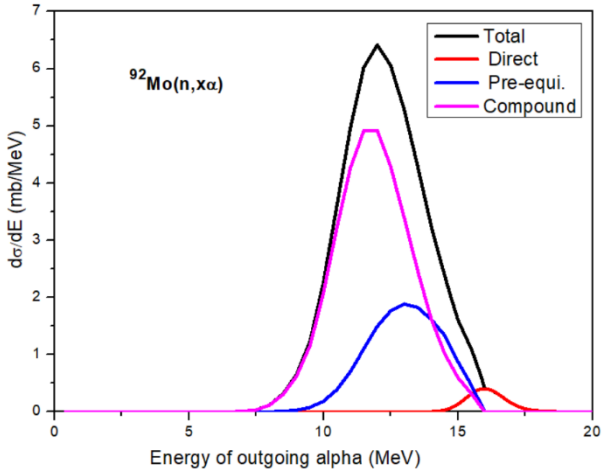

Fig-12: EDX of (n,xα) reaction on ^{92}Mo at 14.1 MeV neutron energy.

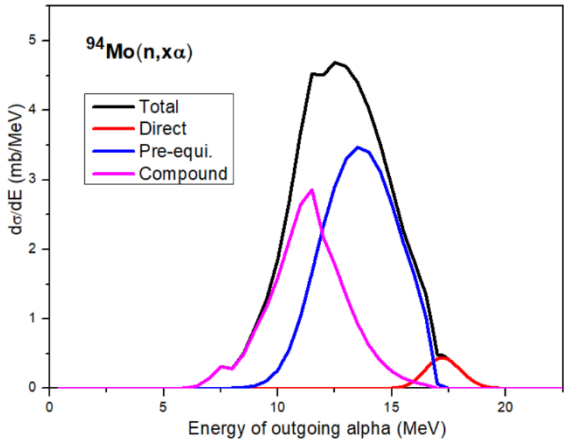

Fig-13: EDX of (n,xα) reaction on ^{94}Mo at 14.1 MeV neutron energy.

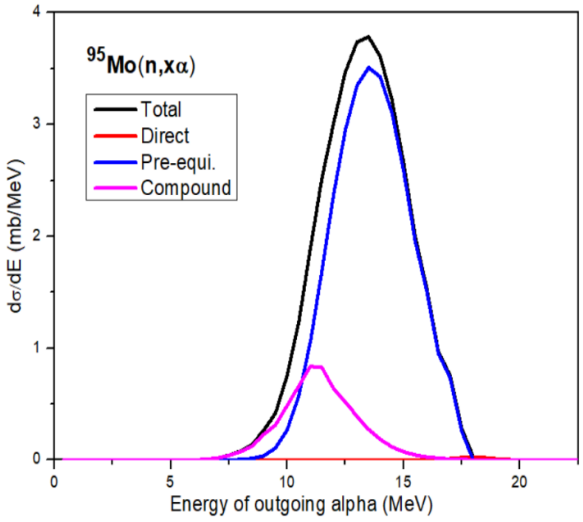

Fig-14: EDX of (n,xα) reaction on ^{95}Mo at 14.1 MeV neutron energy.

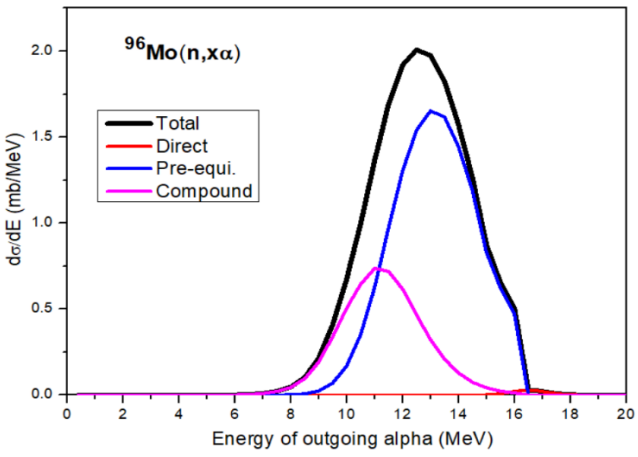

Fig-15: EDX of (n,xα) reaction on ^{96}Mo at 14.1 MeV neutron energy.

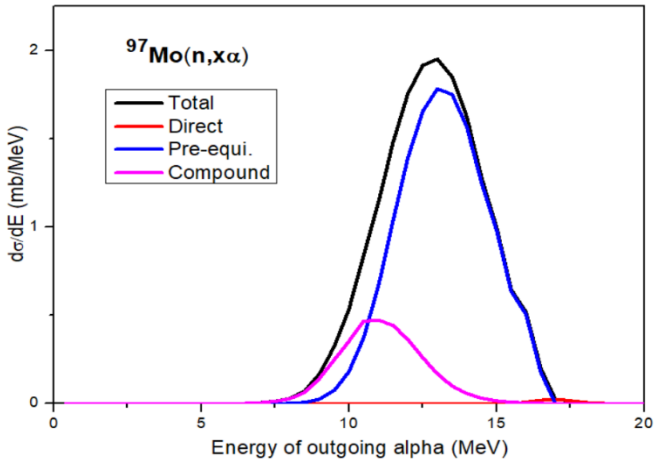

Fig-16: EDX of (n,xα) reaction on ^{97}Mo at 14.1 MeV neutron energy.

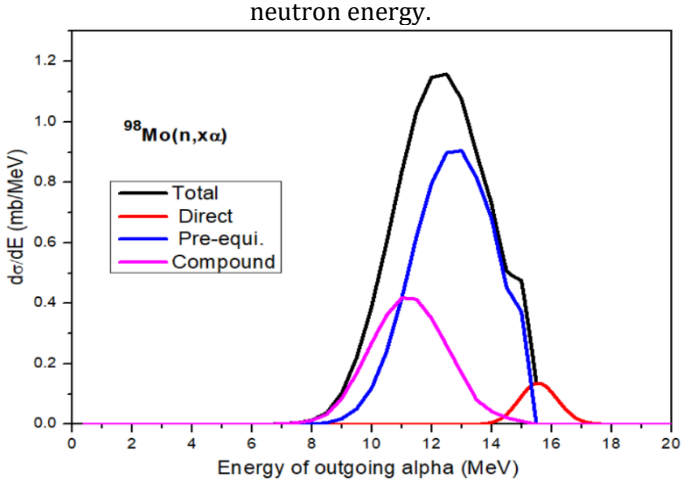

Fig-17: EDX of (n,xα) reaction on ^{98}Mo at 14.1 MeV neutron energy.

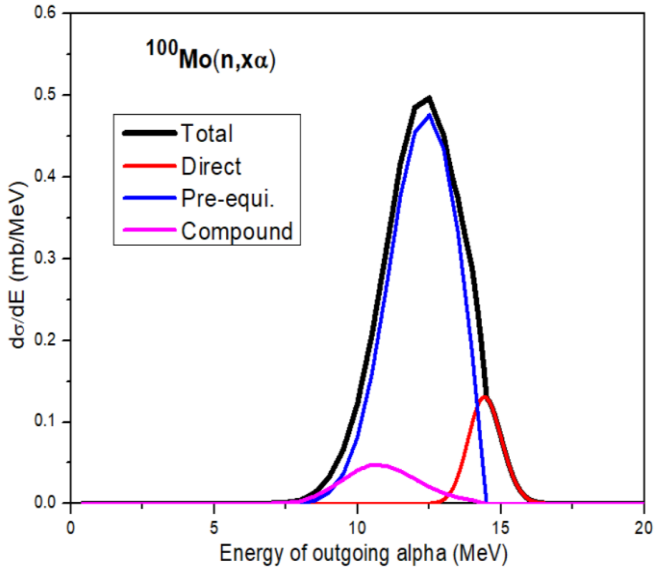

Fig-18: EDX of (n,xα) reaction on ^{100}Mo at 14.1 MeV neutron energy.

3.3. DDX for (n,xp) and (n,xα) reaction on ^{92,94,95,96,97,98,100}Mo

The double differential cross-section ($d^2\sigma/dEd\Omega$) for proton and alpha particles have been calculated for ^{92,94,95,96,97,98,100}Mo at emission angle 10º, 30º,60º, 90º, 120º at 14.1 MeV incident neutrons energy by using TALYS-1.9 code. There is no experimental data available in EXFOR data library for validating theoretical calculation.

The DDX spectra for proton emission at different angles are shown in fig. 19, 20, 21, 22, 23, 24 and 25 for ^{92,94,95,96,97,98,100}Mo. From fig. 19, for ^{92}Mo one can see that the pre-equilibrium reaction is dominant for proton emission whereas contribution of direct and compound nucleus reaction is negligible.

In fig. 20 DDX spectra for emitted proton from ^{94}Mo shows that pre-equilibrium reaction and compound nucleus reaction mechanism play a significant role and the contribution of direct reaction is negligible.

DDX for emitted spectra of proton emitted from ^{95,96,97,98}Mo depicted in fig. 21, 22, 23 and 24 respectively and from the figures it is clear that all three reactions i.e. pre-equilibrium, direct, and compound nucleus reaction contribute significantly to the total DDX but DDX for proton emitted from ^{100}Mo represents that contribution of compound nucleus reaction is negligible, as shown in fig. 25.

The DDX spectra for alpha emission at different angles are shown in fig. 26, 27, 28, 29, 30, 31 and 32 for ^{92,94,95,96,97,98,100}Mo. Fig. 26, 27, 28 and 29 show that alpha particles emitting from ^{92,94,95,96}Mo(n,xα) reaction mainly through compound nucleus and pre-equilibrium rection whereas for ^{97,98,100}Mo alpha particles emitted through pre-equilibrium rection and the contribution of direct reaction and compound nucleus reaction is either low or negligible.

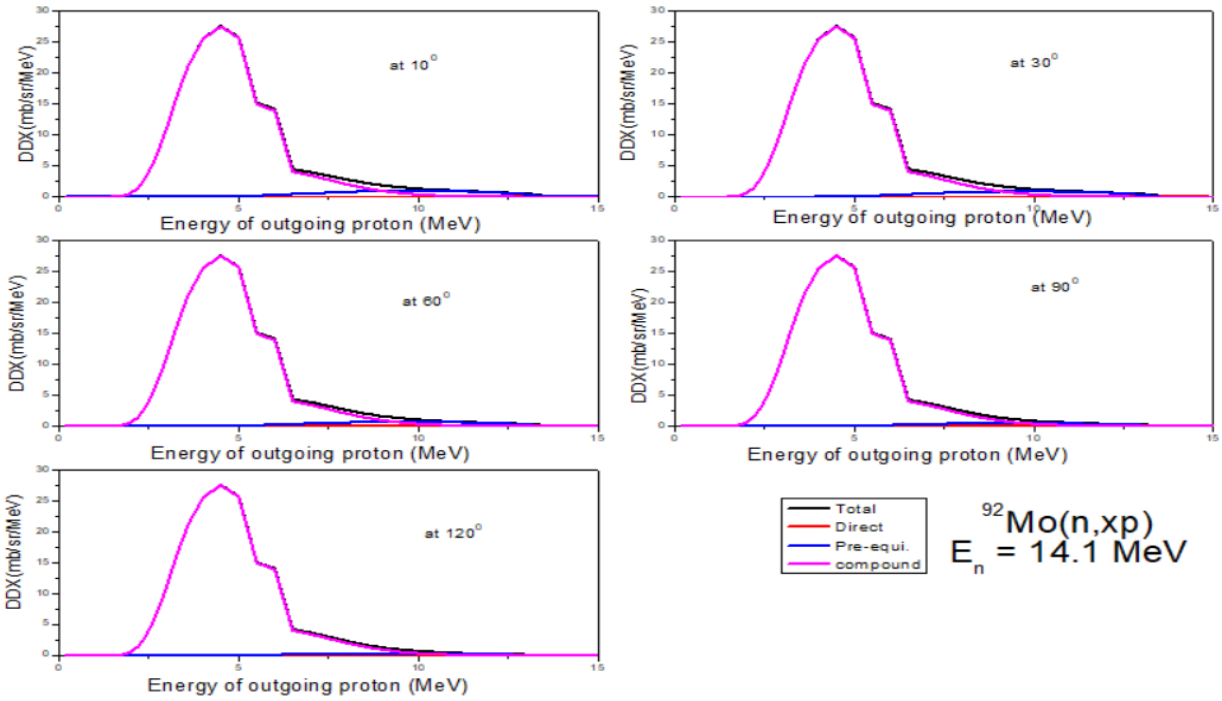

Fig-19: DDX of ^{92}Mo(n,xp) reaction at 14.1 MeV neutron energy at 10º, 30º, 60º, 90º and 120º

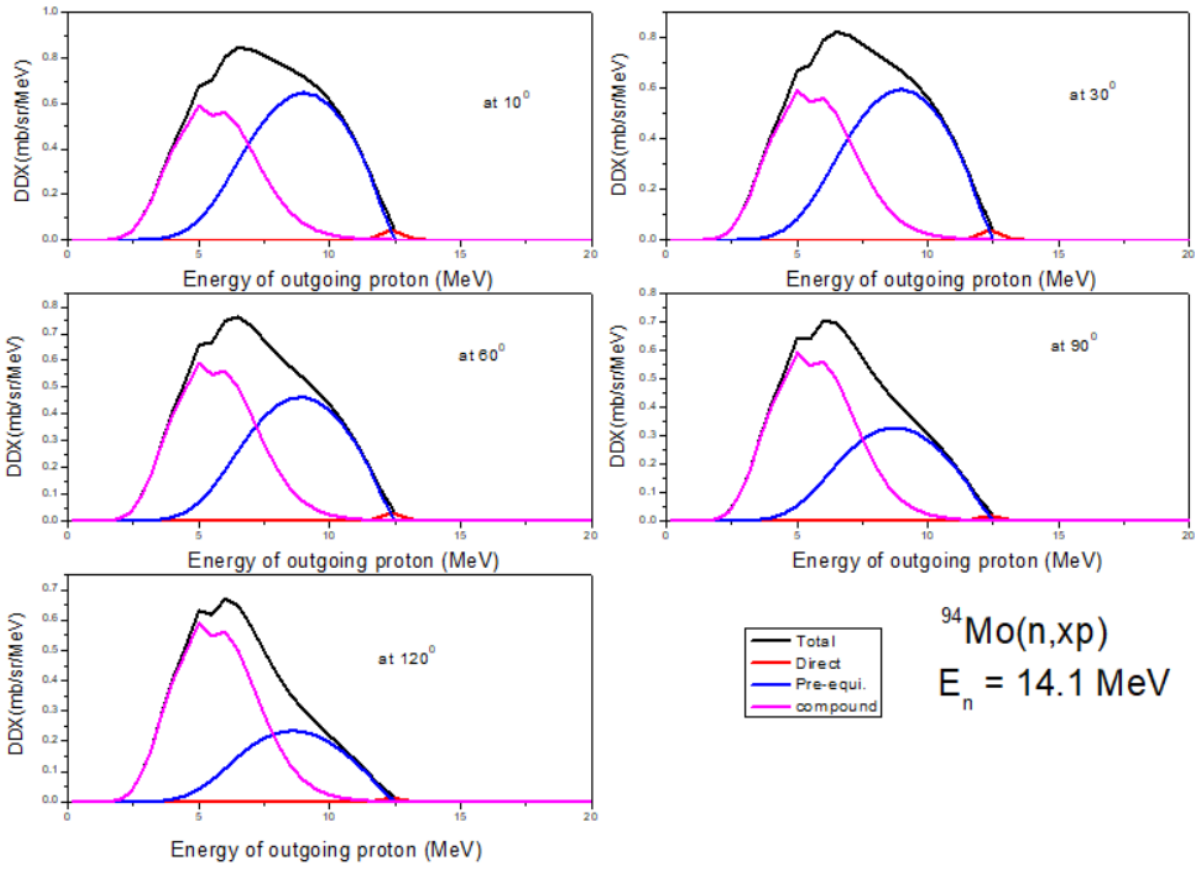

Fig-20: DDX of ^{94}Mo(n,xp) reaction at 14.1 MeV neutron energy at 10º, 30º, 60º, 90º and 120º.

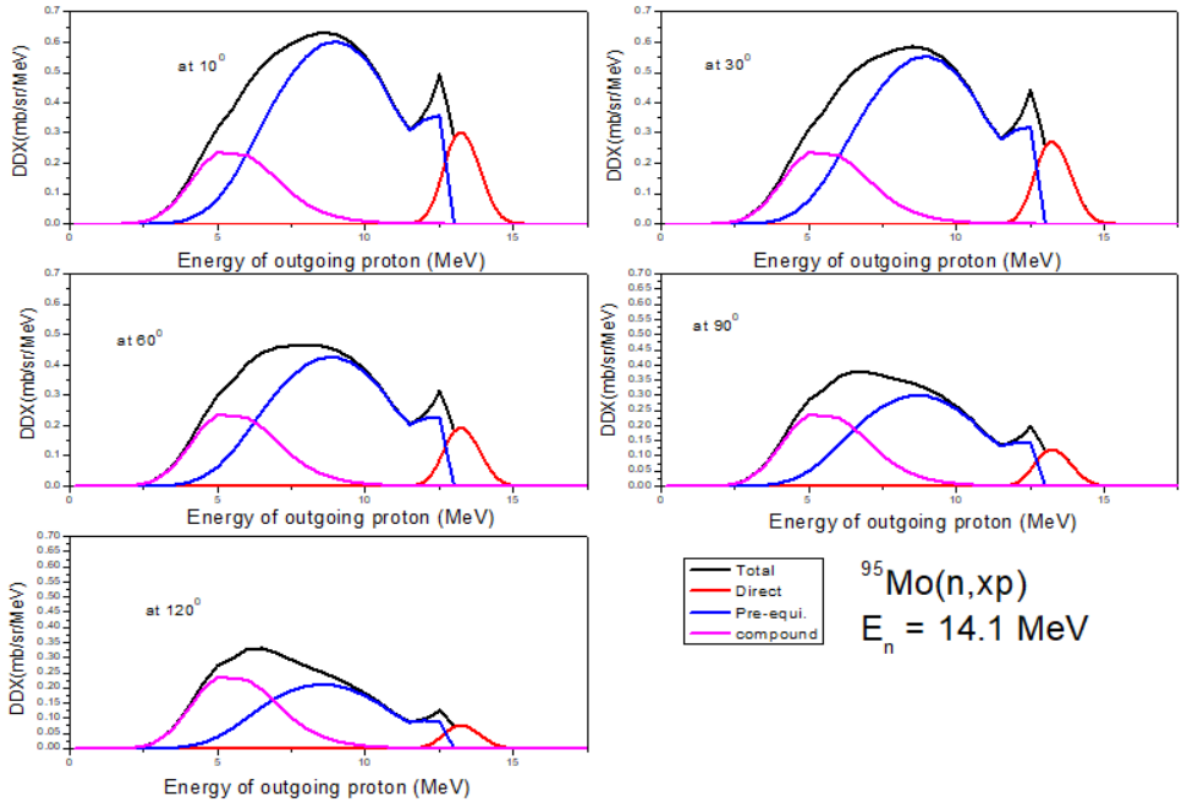

Fig-21: DDX of ^{95}Mo(n,xp) reaction at 14.1 MeV neutron energy at 10º, 30º, 60º, 90º and 120º..

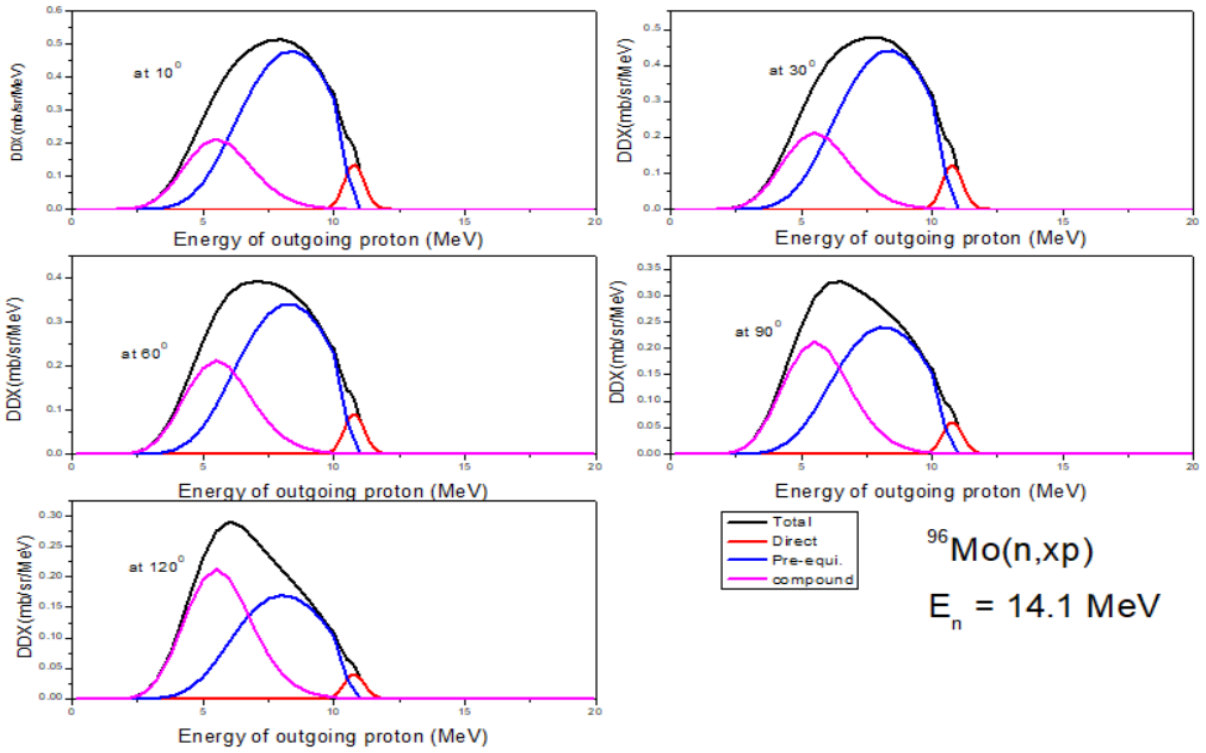

Fig-22: DDX of ^{96}Mo(n,xp) reaction at 14.1 MeV neutron energy at 10º, 30º, 60º, 90º and 120º.

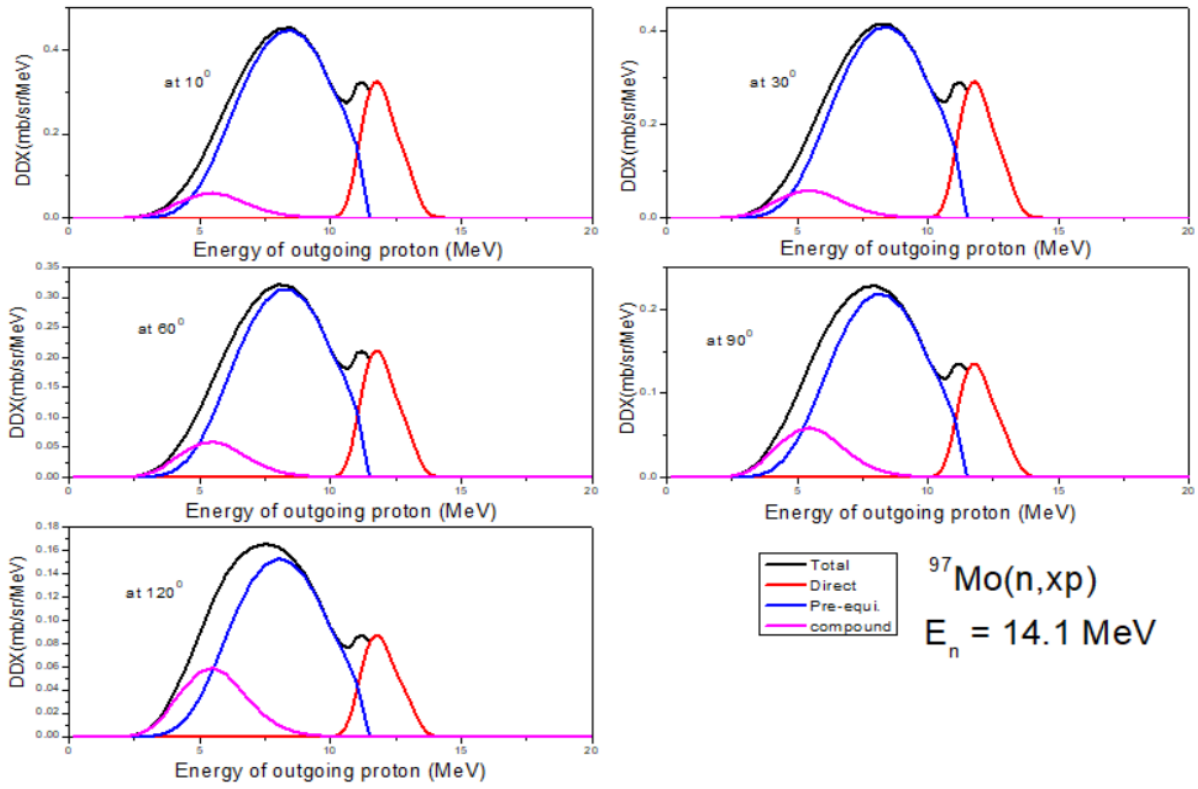

Fig-23: DDX of ^{97}Mo(n,xp) reaction at 14.1 MeV neutron energy at 10º, 30º, 60º, 90º and 120º

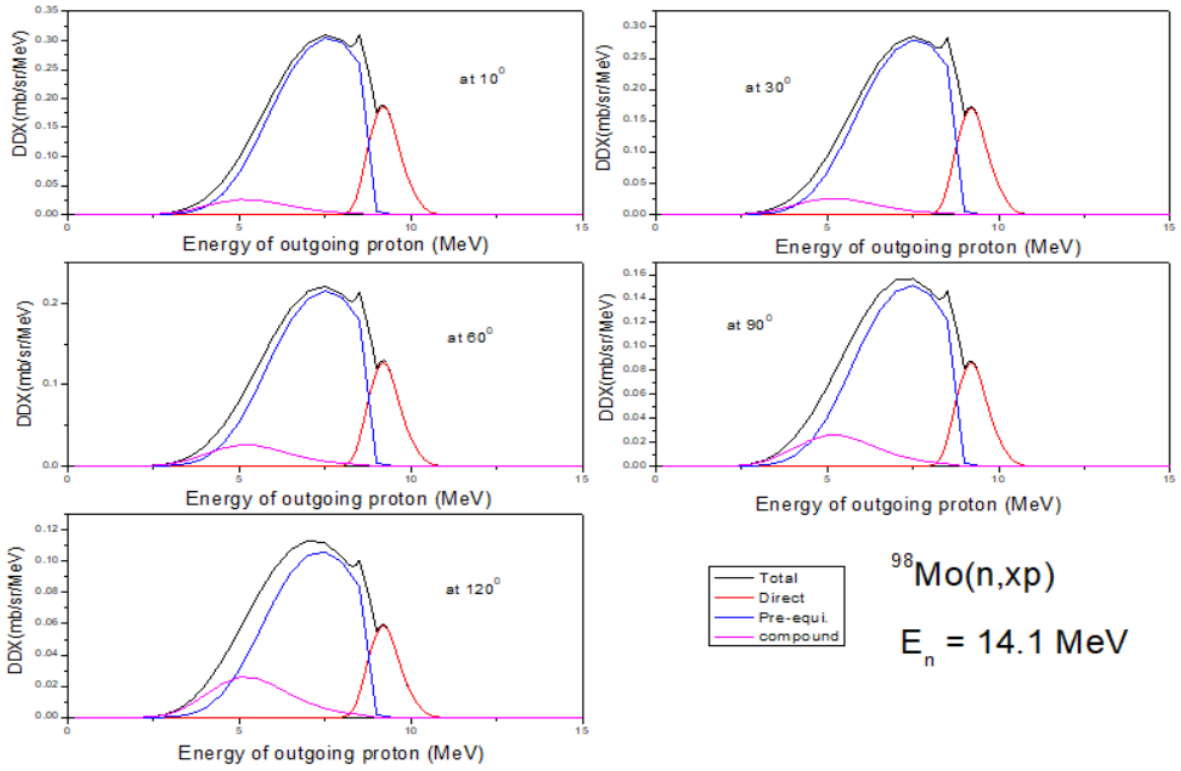

Fig-24: DDX of ^{98}Mo(n,xp) reaction at 14.1 MeV neutron energy at 10º, 30º, 60º, 90º and 120º.

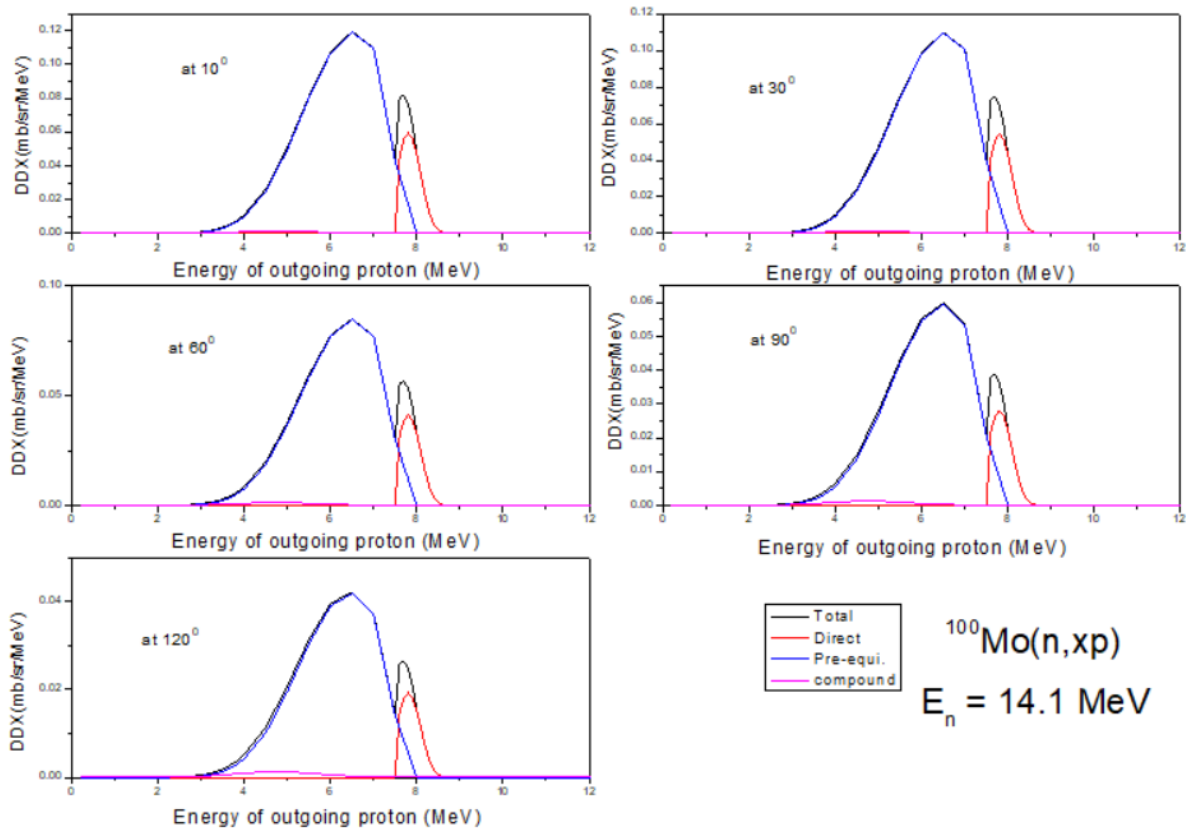

Fig-25: DDX of ^{100}Mo(n,xp) reaction at 14.1 MeV neutron energy at 10º, 30º, 60º, 90º and 120º.

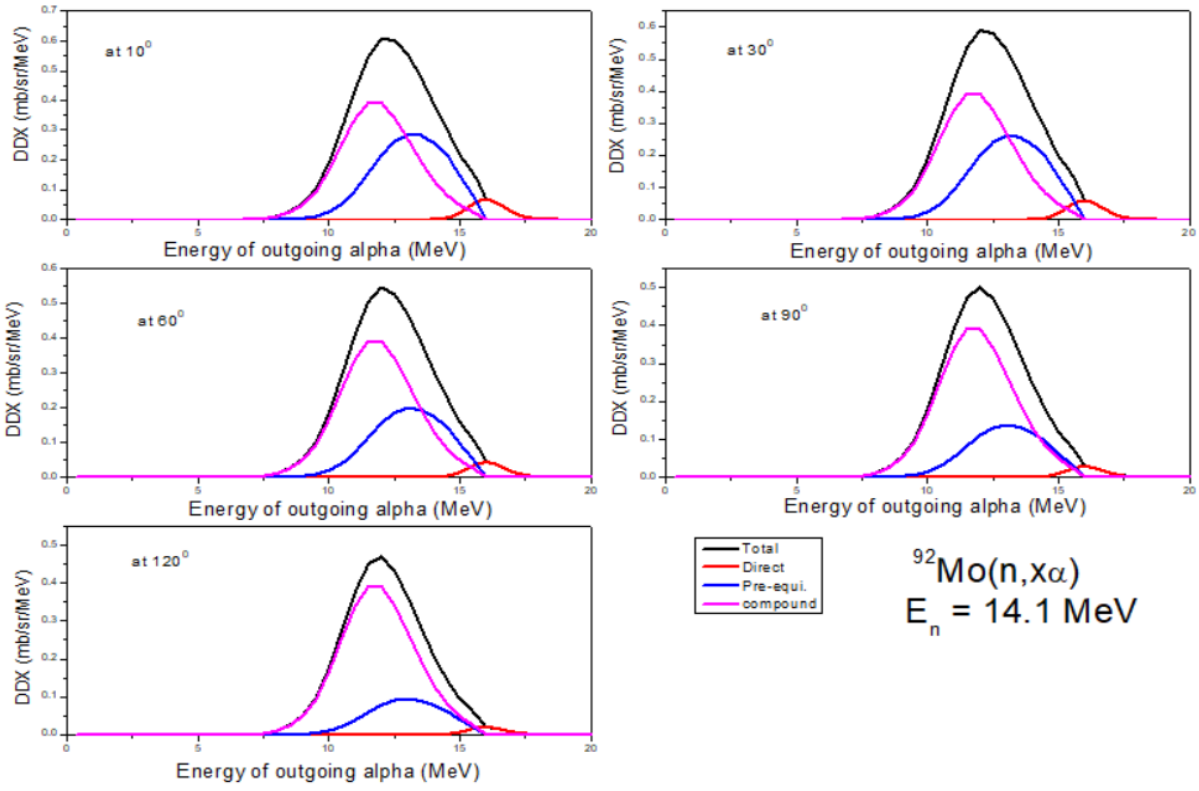

Fig-26: DDX of ^{92}Mo(n,xα) reaction at 14.1 MeV neutron energy at 10º, 30º, 60º, 90º and 120º.

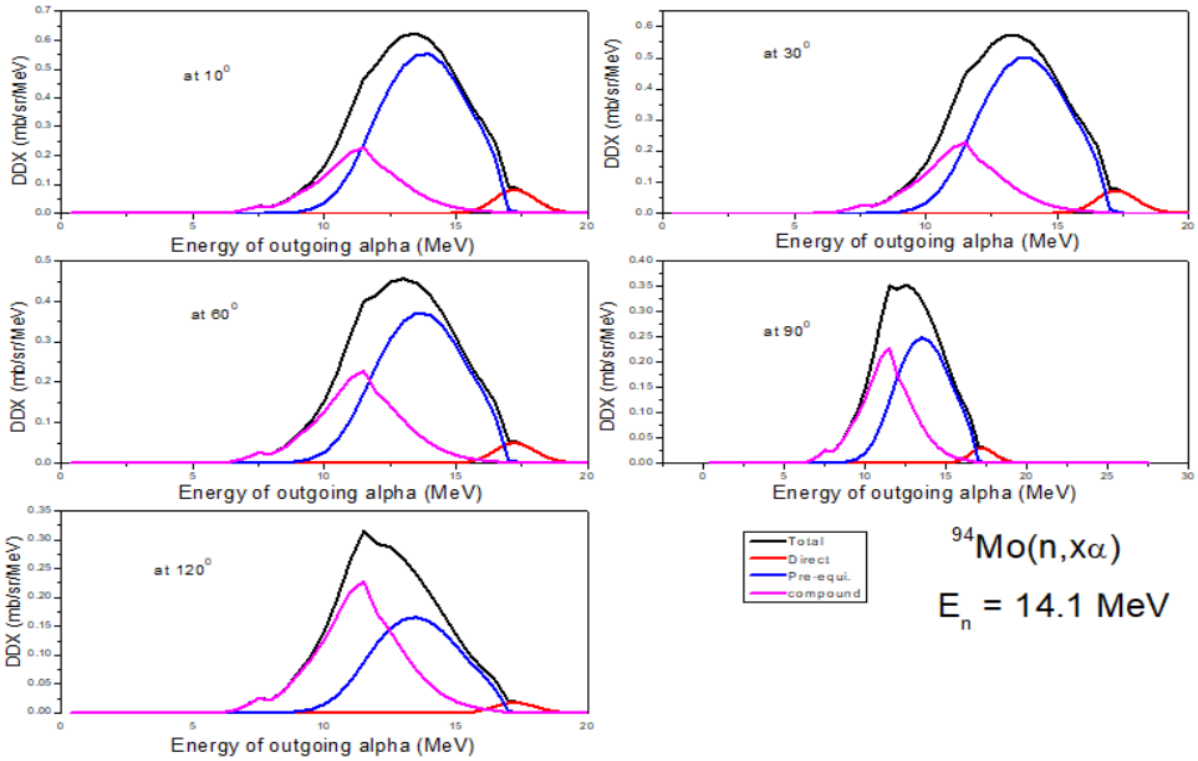

Fig-27: DDX of ^{94}Mo(n,xα) reaction at 14.1 MeV neutron energy at 10º, 30º, 60º, 90º and 120º.

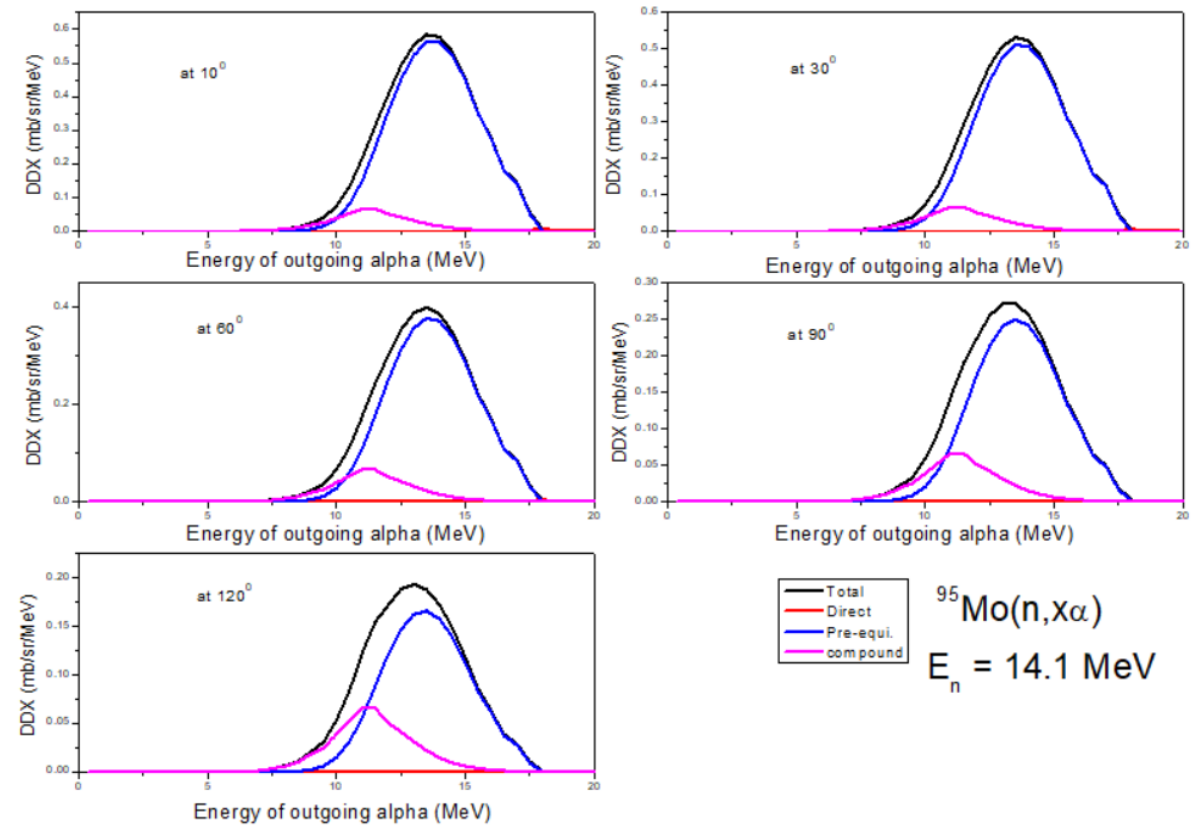

Fig-28: DDX of ^{95}Mo(n,xα) reaction at 14.1 MeV neutron energy at 10º, 30º, 60º, 90º and 120º.

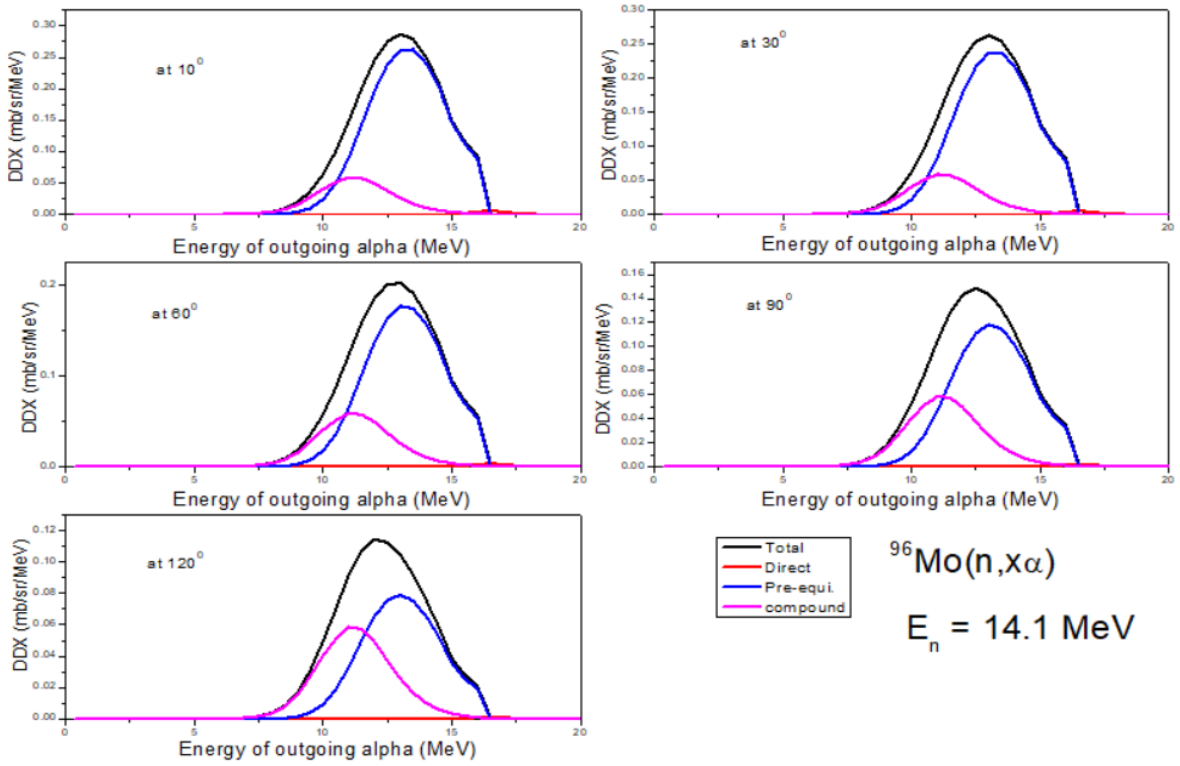

Fig-29: DDX of ^{96}Mo(n,xα) reaction at 14.1 MeV neutron energy at 10º, 30º, 60º, 90º and 120º**.**

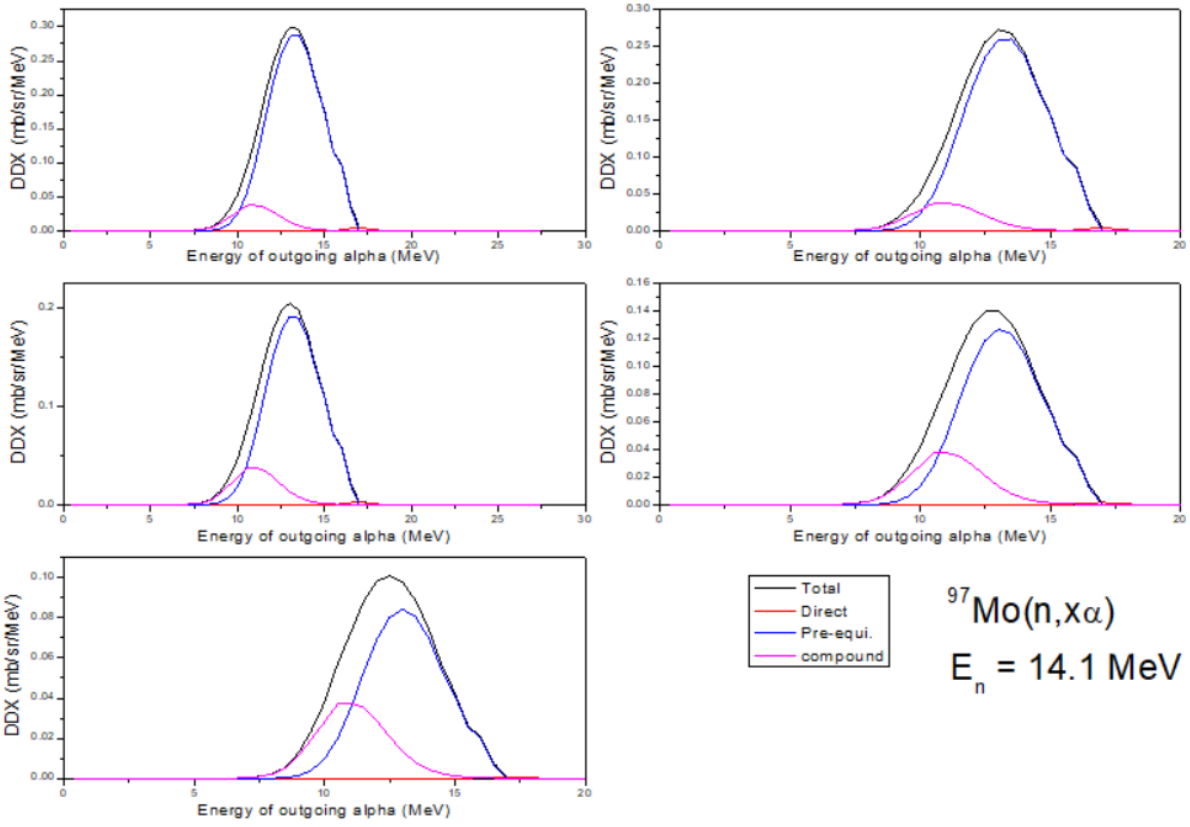

Fig-30: DDX of ^{97}Mo(n,xα) reaction at 14.1 MeV neutron energy at 10º, 30º, 60º, 90º and 120º**.**

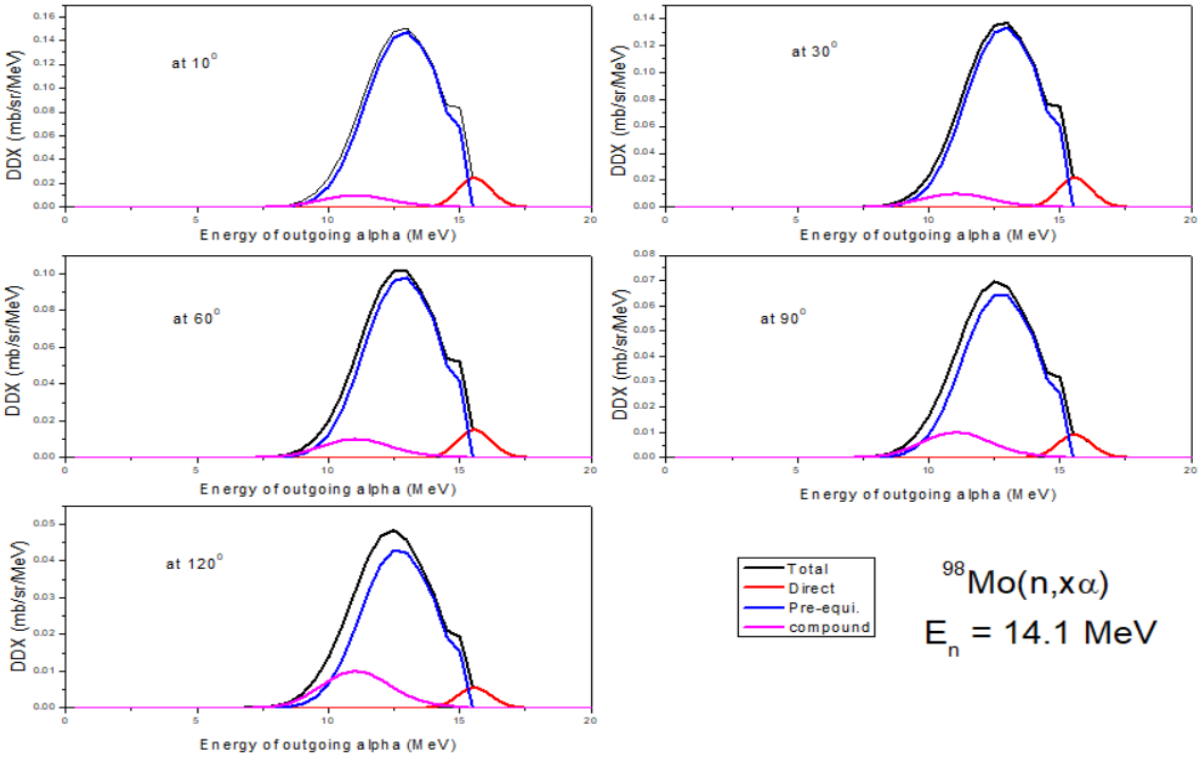

Fig-31: DDX of ^{98}Mo(n,xα) reaction at 14.1 MeV neutron energy at 10º, 30º, 60º, 90º and 120º.

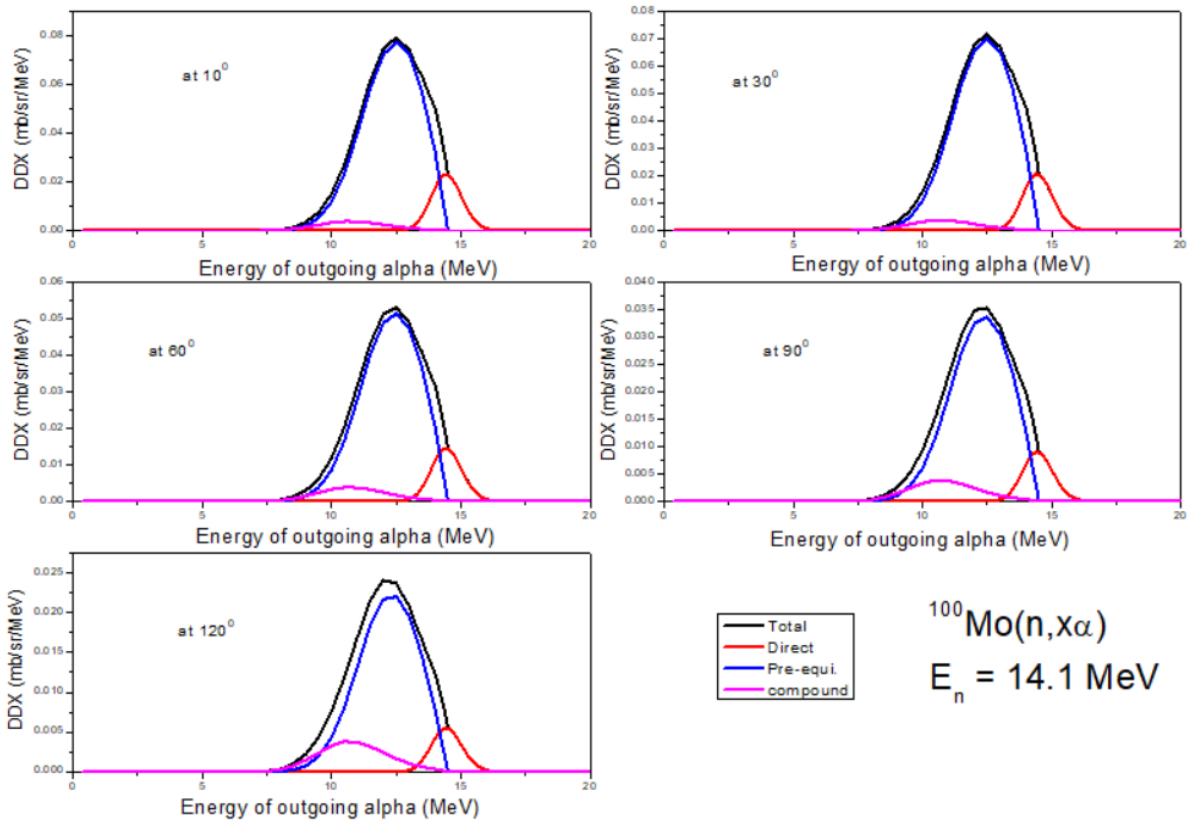

Fig-32: DDX of ^{100}Mo(n,xα) reaction at 14.1 MeV neutron energy at 10º, 30º, 60º, 90º and 120º.

3.4. EDX and DDX spectra for ^{Nat}Mo(n,xp) and ^{Nat}Mo(n,xα) reactions

The aim of the present study is to calculate EDX and DDX for (n,xp) and (n,xα) reactions on natural Molybdenum at 14.1 MeV neutrons energy. The EDX and DDX for (n,xp) and (n,xα) reaction channels are calculated for ^{92,94,95,96,97,98,100}Mo. Isotopic abundance and calculated EDX, DDX of stable isotopes of molybdenum are used to estimate EDX and DDX data for natural molybdenum.

From fig. 33 and 34, it is obvious that the most probable energy of outgoing protons and alpha particles due to 14.1 MeV energy neutrons is about 5 MeV and 13 MeV respectively. There is no experimental data available for energy differential of (n,xp) and (n,xα) reaction channels at 14.1 MeV energy of incident neutrons.

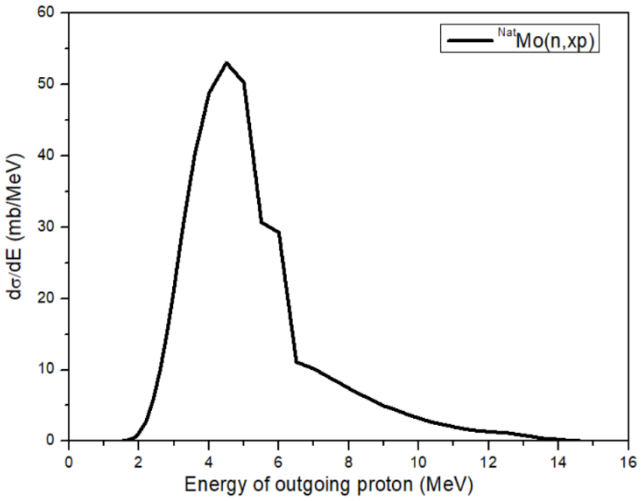

Fig-33: EDX of (n,xp) reaction on ^{Nat}Mo at 14.1 MeV neutrons energy.

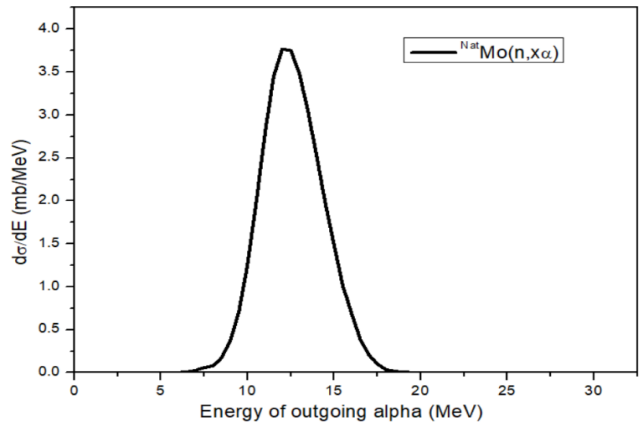

Fig-34: EDX of (n,xα) reaction on ^{Nat}Mo at 14.1 MeV neutrons energy.

For incident neutron energy 14.1 MeV, the DDXs ($d^2\sigma/dEd\Omega$) for the emitted proton and alpha particles has been calculated using TALYS 1.9 for natural molybdenum at five different emission angles i.e., 10º, 30º, 60º, 90º and 120º which is represented in fig. 35 and 36. There is no experimental DDX data available in EXFOR data library with which it can be compared. The alpha and proton emission from ^{Nat}Mo target nuclei has nearly almost isotropic distribution.

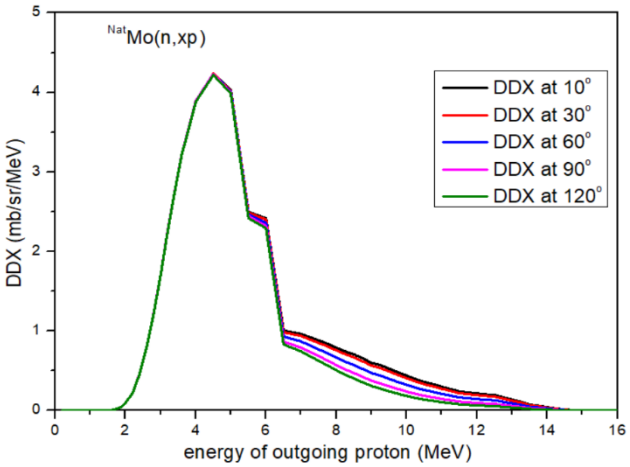

Fig-35: DDX of (n,xp) reaction on ^{Nat}Mo at 14.1 MeV neutrons energy.

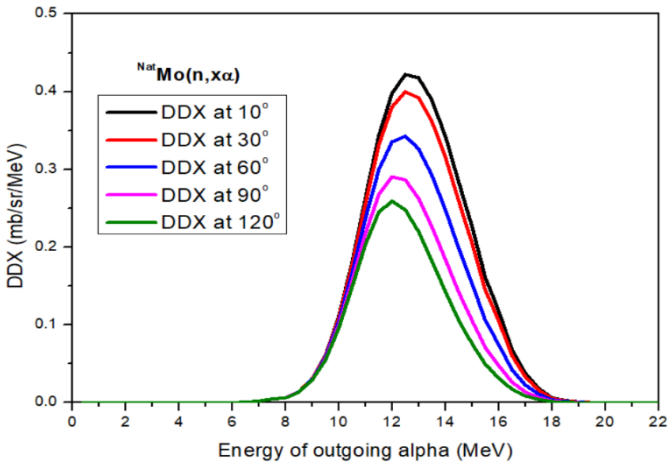

Fig-36: DDX of (n,xα) reaction on ^{Nat}Mo at 14.1 MeV neutrons energy.

4. CONCLUSIONS

Energy differential cross-section (EDXs) and double differential cross-sections (DDXs) data of emitted proton and alpha particles induced by (n,xp) and (n,xα) nuclear reactions for the natural molybdenum plasma facing material at 14.1 MeV neutron energy have been calculated at

10º, 30º, 60º, 90º and 120º angles using TALYS-1.9 and the following conclusions have been derived from the current research study. This can be summarized as follows:

- In the current study, (n,xp) and (n,xα) reaction EDX and DDX for the natural Molybdenum is calculated using versatile nuclear modular code TALYS-1.9 at neutron energy 14.1 MeV.
- The goal of the computation was to determine how much the pre-equilibrium, compound nucleus and direct reaction mechanisms contributed to the total reaction cross-section.
- DDXs are evaluated in various angles which show that more particles released in the forward direction.
- The proton and alpha particle emission from the ^{Nat}Mo target nuclei are almost isotropically distributed.
- For all the angle considered from 10º to 120º, there is a proton peak around 5 MeV.
- For all the angle considered from 10º to 120º, there is alpha peak around 13 MeV.
- These calculated EDX and DDX data can be use to predict nuclear heating, gas production per atom (GPA) and displacement per atom (DPA) in Molybdenum.

REFERENCES

[1] H.Bolt, V. Barabash, W.Krauss., J. Linke, R. Neu., S.Suzuki, "Materials for the plasma-facing components of fusion reactors," Journal of nuclear materials, vol. 329, 2004, pp.66-73, doi: 10.1016/j.jnucmat.2004.04.005.

[2] H. liskien, R. Wolfe, R. Widera and S. M. Qaim, "Excitation functions of (n,p) and (n,α) reactions on molybdenum isotopes," International journal of radiation applications and instrumentation, vol. 41(1) pp. 83-90, doi: 10.1016/j.jnucmat.2004.04.005

[3] W.Z. Yaoa, S.X. Song, Z.J. Zhou , W.W. Cong, Y. Ma , C.C. Ge, "Study on the plasma-sprayed molybdenum as plasma Facing Materials in Fusion Reactor, " Key Engineering Materials, Vol. 373, 2008, pp. 81-84, doi: 10.4028/www.scientific.net/KEM.373-374.81

[4] B. Demir, I. H. Sarpun, A. Kaplan, V. C¸ apalı, A. Aydın, E. Tel, "Double differential cross section and stopping power calculations of light charged particle emission for the structural fusion materials, " Journal of Fusion Energy , vol. 34(4), 2015, pp. 808-816.

[5] G. A. Cottrell, "Sigma phase formation in irradiated tungsten, tantalum and molybdenum in a fusion power plant. Journal of nuclear materials," Journal of nuclear materials, vol. 334(2-3), 2004, pp. 166-168

[6] P. Reimer, V. Avrigeanu, S. V. Chuvaev, A. A. Filatenkov, T. Glodariu, A. Koning, A. J. M. Plompen, "Reaction mechanisms of fast neutrons on stable Mo isotopes below 21 MeV," Physical Review C, vol. 71(4), 2005, 044617, doi. 10.1103/PhysRevC.71.044617

[7] R. Capote, A. Trkov, M. Sin, M. W. Herman, and E. Sh. Soukhovitskii, EPJ Web of Conf. 69, 00008 (2014).

[8] A. J Koning, S. Hilaire & S. Goriely, (2017). TALYS-1.9, a nuclear reaction program (NRG-1755 ZG Petten, The Netherlands).

[9] A. J. Koning and D. Rochman, "Modern nuclear data evaluation with the TALYS code system," *Nuclear data sheets*, VOL. *113*(12), 2012, 2841-2934.

[10] C. Kalbach, "Systematics of continuum angular distributions: Extensions to higher energies," Physical Review C, vol. 37(6), 1988, P2350, doi: 10.1103/PhysRevC.37.2350

[11] Kalbach User's Manual for PRECO-2006 (Triangle Universities Nuclear Laboratory report) 15 (2007)